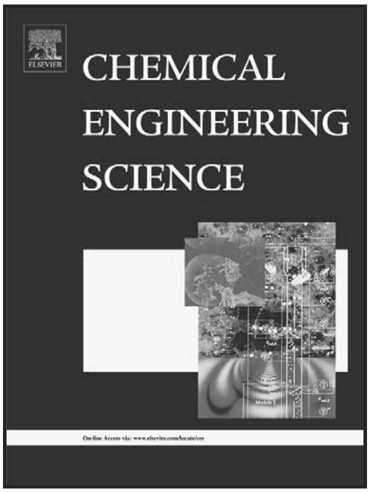

www.elsevier.com/locate/ces

Mixed matrix membranes of 6FDA-6FpDA with surface functionalized γ-alumina particles. An analysis of the improvement of permselectivity for several gas pairs

A. Tena, L. Fernández, M. Sánchez, L. Palacio,
A.E. Lozano, A. Hernández, P. Prádanos

PII: S0009-2509(09)00868-9
DOI: doi:10.1016/j.ces.2009.12.023
Reference: CES 8960

To appear in: *Chemical Engineering Science*

Received date: 13 August 2009
Revised date: 16 December 2009
Accepted date: 18 December 2009

Cite this article as: A. Tena, L. Fernández, M. Sánchez, L. Palacio, A.E. Lozano, A. Hernández and P. Prádanos, Mixed matrix membranes of 6FDA-6FpDA with surface functionalized γ-alumina particles. An analysis of the improvement of permselectivity for several gas pairs, *Chemical Engineering Science*, doi:10.1016/j.ces.2009.12.023

Mixed matrix membranes of 6FDA-6FpDA with surface functionalized γ-alumina particles. An analysis of the improvement of permselectivity for several gas pairs.

A. Tena[2,4], L. Fernández[1], M. Sánchez[1], L. Palacio[2,4], A.E. Lozano[3,4], A. Hernández[2,4] and P. Prádanos[2,4]

[1] *Dpto de Química, Facultad de Ingeniería, Universidad Nacional del Comahue, Buenos Aires 1400 - 8300, Neuquén. Argentina*
[2] *Dpto. Física Aplicada, Facultad de Ciencias Universidad de Valladolid, Real de Burgos s/n, 47071 Valladolid. España.*
[3] *Instituto de Ciencia y Tecnología de Polímeros, CSIC, Juan de la Cierva 3, 28006 Madrid. España.*
[4] *Surface and Porous Materials (SMAP), UA-CSIC-UVA, R&D Building, Belén s/n, Campus Miguel Delibes. 47071 Valladolid. España.*

Summary

Herein, mixed matrix membranes including alumina particles whose surfaces have been differently modified have been made and characterized. The polymeric matrix is a fluorinated polyimide, 6FDA-6FpDA, whereas the inorganic constituent parts are neat, silanized or poly-vinyl-pirrolidone coated nanometric γ-Al_2O_3 particles of 40 nm in diameter which have been added in an approximated percentage of a 12 % w/w.

All the modified or unmodified added particles leaded to similar improvements in the permselectivity of the gas pairs studied. Only in the case of the O_2/N_2 pair the increase in selectivity for the silanized particles is not as effective as the observed permeability enhancement for the uncoated and PVP coated particles. In the case of CO_2/CH_4, the 1991 Robeson's upper bond line is overpassed.

The characteristics of the permselectivity improvement for the different inorganic particles have been analyzed in terms of the properties of the particle-polymer interfacial properties.

Keywords: Gases, Separations, Membranes, Nanostructure, Permselectivity, Diffusion

1. Introduction

Two of the main contaminant of the natural gas are the CO_2 and N_2, which use to be naturally present in the rocks. In addition, CO_2/CH_4 and N_2/CH_4 separation could be needed as a consequence of using high pressure gases during extraction procedures. Thus, pressurized N_2 is used to increase the recovery of hydrocarbons in some oilfields. In this way, and according to the high cost of oil nowadays the commented separations play a relevant role not only for this secondary oil extraction procedure but also have a relevant role in tertiary oil extraction when the oil viscosity is reduced to increase its production by injecting hot gases into the reservoir or when the carbon dioxide flooding method is used [1]. This method consists in injecting pressurized CO_2

when the natural gas reservoir pressure is depleted through primary and secondary production to take advantage of their very good solvent properties. CO_2 flooding is the second most common tertiary recovery technique and it is use in facilities around the world. CO_2/CH_4 gas separation plays also a very important role in the transport of natural gas through pipelines where sour gases could be very problematic.

The conventional gas treatment plants have byproducts consisting in both liquid and gas fraction. The gas streams contain high proportions of natural gas with some percentages of other non-condensable gases as CO_2, N_2 or others depending on the specific treatment and raw product used. These gases should be eliminated in order to increase the calorific power of such a gas stream. Other applications of the CO_2/CH_4 and N_2/CH_4 gas separations can be found in many processes in refinery, petrochemical processing, etc…[2,3].

In the scope of global warming, CO_2 flooding seems an available method to curb CO_2 emissions, [1]. An extensive use of such a procedure to eliminate CO_2 from the emissions of power plants should need several gas separation steps including the CO_2/N_2 one.

Membranes can be used to recover methane from biogases such as landfill which composition of N_2 and CO_2 can be high. These separations can also play a relevant role to control the composition of several pyrolytic and cogeneration gaseous streams, [4]. In direct conversion of biomass to hydrocarbons, N_2 and CO_2 need to be separated from light hydrocarbons.

On the other hand, there is a big market for the O_2/N_2 separation to obtain NEA (nitrogen enriched air) and/or (oxygen enriched air) OEA, mainly to improve the coal burning in thermal power plants, [5]. These applications include the obvious medical ones but also some applications in the industry where the oxidizing or inert character of a gaseous stream has to be tuned, [3, 6]. An example of such kind of applications is the control of the process of pyrolysis of biomass, [4]

At present, membranes for gas separations are an interesting alternative by using polymeric materials. Nevertheless, there are a number of possible itineraries addressed to improve the permeability and selectivity of gas separation membranes. One of them tries to optimize the structure of the polymer chains to give high volume fractions with restrictive or selective channels communicating the voids in order to increase the diffusivity. Other possible approach consists of attempting to increase the solubility introducing a certain chemical affinity for a gas to make it to adsorb on certain moieties of the polymer. An alternative and promising line involves the addition of inorganic micro or nano-particles in a polymeric matrix whose permselective properties were already good in order to improve them yet more, [7,8]. These resulting membranes are called mixed matrix membranes.

Apart from the contribution of both the bulk phases, inorganic and polymeric materials, the interfaces between such phases play a relevant role. Herein, we are obtaining mixed matrix membranes that include several inorganic particles differently coated in order to modify the resulting polymer-particle interfaces. Our aim has been to compare theses systems to separate N_2/CH_4, CO_2/CH_4, CO_2/N_2 and O_2/N_2 and also to figure out how they improve the characteristics of the neat polymeric matrix.

The incorporation of filling materials can increase or decrease the transport of one or several gases through the mixed matrix membrane when compared to that of the polymeric matrix alone. Obviously, the shape, the size and the chemical nature of the filling particles plays a key role on the transport properties.

The transport, i.e. the permeability and or the selectivity can get better because:

- The particles inserted within the polymeric matrix present better permeability or selectivity than the polymeric matrix in such a way that the addition of their properties lead to better overall transport properties, [7, 9-11].

- The characteristics of the interface between the filling material and the polymer could increase or decrease the path to be traveled by one of the gases over the rest of them. This should increase the selectivity, or it could decrease the length to be covered by all the gases, which should increase the permeability, [12].

- The particles could modify the properties of the neighbor polymer phase which should favor its permeability or its selectivity [13, 14]. In some cases, for particles very well distributed or spread within the polymeric matrix, the modifications of fractional free volume could affect the polymeric phase, [15-17].

When particles with very good permselective properties, as for example zeolites, are used as fillers, better selectivities are obtained while permeability does not necessarily increase [18]. When there is a better compatibility of the particles with the polymeric matrix, as for example when active carbon is used, there exists a simultaneous improvement of selectivity and permeability [7]. For non permeable particles an increase in permeability leads to a decrease in selectivity, especially when there is also a lack of adhesión of filler and matrix [19]. This effect is more remarkable when a pair of lowly condensable gases is used. If both the gases are highly condensable, as for example n-butane/methane both permeability and selectivity increase by using silica particles in a PMP matrix [20].

Here the *6FDA-6FpDA* polymer, Figure 1, has been modified by the incorporation of γ-alumina particles with a nominal diameter in the range from 45 to 50 nm. The particles were included without any modification or with different moieties covalently bonded to their surfaces. The grafted materials were a silane network and a poly-vinyl-pyrrolidone attached to the surface through a silane link, [21]. In our case the neat particles are dense and cannot be penetrated by any of the gases studied. Thus their effect could consist only in: a) modification in the permeability or selectivity of regions of the polymeric matrix due to a distortion of its structure induced by the particles, b) increase or decrease in the path to be followed by the gas through the membrane due to the specific solubility (the coating could introduce some chemical affinity) or c) changes in diffusivity (modifications in the free volume) at the interface between the polymer and the particle surface. We will see how, in our case, the permeability increases without a simultaneous decrease and sometimes with a moderated increment of selectivity. How those mechanisms act for the diferent gases and particles used will be analyzed below.

2. Experimental

Polymer matrix

The polymer chosen to constitute the polymeric matrix of our mixed matrix membranes is the *6FDA-6FpDA*, made from 4,4’-(hexafluoroisopropylidene)diphthalic Anhydride (6FDA) and 4,4’-(hexafluoroisopropylidene)dianiline (6FpDA), which chemical structure is shown in Figure 1. *6FDA-6FpDA* is a fluorinated polyimide presenting by itself good gas separation properties, [22-24], good mechanical, thermal and transport properties, [25]. It also shows an appreciable resistance to plasticization, [26].

This polyimide was synthesised by us following the classical in situ silylation two steps method from the 6FpDA diamine and the 6FDA dianhydride, [27-29]. The intrinsic viscosity of the so obtained polymer is 0,62 dL/g.

Inorganic nanoparticles

The used γ-alumina particles were: (a) untreated, (b) silanized and (c) coated with poly-vinyl-pyrrolidone (PVP) attached through a silane linker. The particles of γ-alumina ((γ-Al_2O_3) are non-porous ones with average diameters from 45 to 50 nm according to the specifications given by the manufacturer (Sigma, CAS 1344-28-1).

The particles have been silanized by the method described by Yoshida et al. [30]. In a 500 mL reactor, a 80 g/L water solution of the particles was added on a 10% (v/v) solution of vinyl-trimethoxysilane (VTMS) (Fluka, 95095) in a mixture of isomers of xylene (Fluka, 9560). The mixture was kept at 130 ºC and stirred during 5 hours. The vapors produced are condensed at 75 ºC and the produced methanol was stripped off. A scheme of the reaction is shown in Figure 2-A.

Once the nanoparticles were silanized, they were coated with PVP by two consecutive steps. The process consists in a hydrolysis of the methoxy groups followed by a polymerization of the vinyl group. The hydrolysis is achieved by keeping the silanized γ-alumina particles during 3 days in a stirred NaOH aqueous solution at pH 9.5 and ambient temperature. In Figure 2-B the so produced reaction of hydrolysis is shown. Afterwards, 1-vinyl-2-pyrrolidone (Fluka, 95060) was free-radical-polymerized in an aqueous medium with the silanized and hydrolyzed particles. The reaction was started by a 30 % water solution of oxygen peroxide with a water solution of ammonia

(24º Be) as co-catalyst in a reactor under a nitrogen atmosphere to reduce the latency period and to increase the rate of polymerization. 5 g of hydrolyzed particles were poured and dispersed in 200 mL of the co-catalysts solution and kept at 70 ºC (due the exothermic behavior of the reaction, its refrigeration is required). Finally, the reaction was stopped by adding Milli-Q treated water. The reaction is shown in Figure 2-C.

The productivity of the reactions was evaluated by Thermogravimetry (TGA) leading to 0.48 mg/m^2 for the sylilation and to 2.31 mg/m^2 for the polymerization, [21]. The silanized particles were washed with the xylene solvent and then recovered by rota-evaporation. The PVP covered particles were separated from the unlinked PVP by centrifugation.

The size of the particles has been determined from the specific surface area (BET area) and the density of all the materials constituting the core and the deposited layers by assuming pure spherical geometry. The BET area was evaluated by using the Brunauer-Emmett-Teller theory and the nitrogen adsorption isotherms at 77 ºC determined in an Omnisorp 100 CX by Coulter®. The values for the surface area (S_S) and the diameter of the particle (d_p) are shown in Table I. It is clearly seen that the surface area decreases when more and more PVP layers are added. On the other hand, the size of the alumina particles is very similar to that given by the manufacturer, with a slight increment for the silanized ones and a more substantial growth in diameter after the PVP coating, [21]. Figure 3 shows the three types of particles obtained after the treatment.

Membrane Manufacture

The membranes were manufactured by using tetrahydrofuran (THF) as solvent, stabilized with 250 ppm of 2,6-Di-tert-butyl-4-methylphenol (BHT). A 15% w/v solution of the polymer in THF was mixed with the same volume of a 2% w/v suspension of the particles in THF. The solution of polymer was prepared by vigorous stirring and filtered with a 1 µm (Titan, PTFE) membrane. The suspension was made by treating the combined solution and suspension with ultrasounds by means of a sonic horn.

The films were obtained by the method of casting on a levelled glass plate kept at 25 ºC. Afterwards they were kept at 60 ºC during 12 hours and later at 80 ºC for 1 hour in order to completely eliminate the solvent. The so obtained films were separated from the glass by immersion in distilled water and introduced in a vacuum oven at 180 ºC where they were maintained for 24 hours. The used proportion of particles obtained is shown in Table II. After these treatments the membranes were ready to measure their permeabilities for different gases and to evaluate the corresponding permselective properties. Images, obtained by SEM, of cross sections of the membranes with and without the filling particles, are shown in Figure 4. It is easily seen that there is a worst adherence of the polymer and the particles when they are uncovered.

Measurements of Permeability

The permeability, P, for the N_2, CO_2 and CH_4 gases has been determined by using a permeator with constant volume and variable pressure which uses the “time lag” operation method. The measurements have been carried out at 3 bar and 30ºC, [7]. In Figure 5 a drawing of the used device is shown.

The strategy of the known as “time lag” method is attributed to Daynes, [31], and it is able to determine permeability, diffusivity and solubility of a sample by a simple, rapid and smart method working under transitory regime. The method was successfully applied to polymer permeation by Paul and DiBenedetto, [32], Crank, [33], and Barrer and Skirrow, [34]. It is nowadays a classical method to assess the permeability and diffusion coefficients of a gas through a polymer film for a given set of operating conditions (temperature and pressure). To sum up, the classical treatment postulates, among others, Fick's law to hold with a constant diffusion coefficient and constant membrane thickness (i.e. negligible swelling effect exerted by the permeant). When these conditions are prevailing, the transitory response at the downstream part of a membrane to a pressure step at the upstream part enables a characteristic time to be easily computed from experimental data, the time-lag, t_0, (shown in Figure 6). This parameter gives access to the permeant diffusion coefficient, D, through the simple expression, [33]:

$$t_0 = \frac{\Delta x^2}{6D} \tag{1}$$

Δx being the thickness of the membrane.

The amount of gas transmitted at time t through the membrane was calculated from the permeate pressure, p_2, readings in the low-pressure side. The inherent leak rate in the downstream side determined after evacuating the system was measured for each experimental run. The permeability constant can be obtained directly from the flow rate into the downstream volume upon reaching the steady state. The theoretical framework, as well as the practical possibilities and limits of the time-lag technique have been abundantly documented, [36-38]

Finally, solubility, S, can be obtained from directly measured diffusivities and permeabilities as:

$$S = \frac{P}{D} \tag{2}$$

3.- Results and Discussion

In Figures 7.A-D the corresponding Robeson representations of selectivity versus permeability are shown for the gas pairs studied here. Note that, for the CO_2/CH_4 and N_2/CH_4, the inclusion of the silanized particles lead to an increase in selectivity with only a moderate increase in permeability of the most permeable gas in the pair while the unmodified γ-alumina as well as the PVP coated particles lead to high increments in permeability but with a very low effect on selectivity. For the pairs not including methane, i.e. for O_2/N_2 and CO_2/N_2, the permeability for the most permeable gas in the pair is also moderated for the mixed matrix membranes including silanized particles but the selectivity is almost constant. For these pairs of gases, the other mixed matrix membranes, including uncoated γ-alumina or the PVP coated particles, give bigger permeabilities for the most permeable component of the analyzed pair, with the same low effect on selectivity.

In all these figures, the corresponding Robeson's bond lines are shown both as predicted in 1991, [39], and in 2008, [40]. Note that for the pairs N_2/CH_4 and CO_2/N_2 no limits were proposed in the original 1991 work of Robeson. In any case, it is clear that very good results are obtained for the CO_2/CH_4 pair. Moreover, it is worth noting that very similar performances are obtained for all the mixed matrix membranes studied, since all of them surpass the old Robenson's bond. For the other pairs of gases, the results are good enough in all cases but especially for the membranes including PVP coated or unmodified γ-alumina particles mainly due to the high permeabilities reached in these cases. In all these cases (naked and PVP coated particles), increments in permeability around a 50% are obtained for CO_2, N_2, and O_2 and of a 30% for CH_4, with moderate increments in selectivity. Lower increments in permeability are found in literature when non porous fillers are used as for example TiO_2, MgO or ZnO as used by Matteuci et al. with similar percentages to those used here, [19,41,42].

The changes in both the selectivity and the most permeable gas permeability, when including inorganic porous charges (as zeolites for example) into a polymeric matrix have been analyzed by Moore and Koros, [43]. They attribute comparatively large increases in permeability with no or low changes in selectivity owing to a poor adhesion of the polymer to the surface of the particles leaving voids or a high free volume phase forming an *halo* around the particles acting as an interface that do not add any selectivity. When the size of the voids in the *halo* are of the order of the mean free paths of the permeant gases, the permeation across the material of the *halo* follows a Knudsen regime that favours the lighter gas and thus should slightly decrease selectivity. When the size of the voids is similar to the size of the gas molecules both the diffusion and solubility across the voids should be very low and the corresponding solubility should pass through a minimum. On the other hand, when neither the pores in the sieve particles nor the free volume of the polymer are modified, the Maxwell model should predict a simultaneous increase of selectivity and permeability given that the permeabilities are lower and the selectivity is higher across the sieve particles. This behavior has been studied and probed by Chung et al. [44, 45] for particles of zeolite which surface was treated similarly to some of these used here. They have also studied how the membrane morphology influence in the mixed matrix membrane performances, [46]

In our case we have the same two kinds of modifications but our γ-alumina particles cannot be considered as sieves but rather as compact impenetrable phases. Moreover, in some cases we have coating layers that can modify strongly the properties of separation. Actually, what we think that is probably happening is:

i. When we add uncoated γ-alumina particles, the adherence with the 6FDA-6FpDA is poor (see figure 4) and the voids left are bigger than the sizes of the penetrant gases leading to an increase in permeability because the path of all the gases across the polymer is reduced.

ii. When the PVP coated membranes are used, the PVP shell act as a high free volume interface and possibly disturbs the 6FDA-6FPDA matrix to increase its free volume. In this case the effect should be also a decrease in the effective length of selective membrane to be crossed.

iii. Finally when we use silanized γ-alumina, the silane groups interacting with 6FDA-6FpDA should give a selective shell, according to the experimental results, when CH_4 is one of the permeant gases. Thus leading, in this case, to a Maxwell type mixture corresponding to the addition of a more permeable and selective medium to the polymer matrix, [43]. Here, this highly permeable and selective material should be the *halo* formed by the silane and 6FDA-6FpDA chains. It is worth noting that when methane is not one of the penetrating gases, properties are totally different for the silanized particles that behave like those coated with PVP but corresponding to systems with smaller free volumes and leading to not so high increases in permeability but without significant changes in selectivity.

More information on the details of the processes appearing for the different gases can be obtained from their diffusivities and solubilities through the mixed matrix membranes. These parameters can be obtained according to equations (1) and (2). It is known that the diffusivity should decrease with the kinetic diameter of the gas and the solubility with its critical temperature, [47, 48]. The different behaviour of the gases used can be analyzed in terms of their kinetic diameter and critical temperature which are shown in Table III, [49, 50]. The so obtained diffusivities and solubilities follow these general trends with the exception of CO_2 that has a much lower diffusivity should be expected according to its kinetic diameter as it is widely known, [48]. These trends are shown in Figures 8-A and B.

In Figure 9 the solubility selectivity is shown versus the diffusivity selectivity for all the membranes and gas pairs studied, defined as

$$\alpha_{ij} = \frac{P_i}{P_j} = \frac{D_i S_i}{D_j S_j} = \alpha_{ijD}\alpha_{ijS} \tag{3}$$

It can be seen that, for all the membranes, N_2/CH_4 is the gas pair with the most diffusive selectivity followed by CO_2/CH_4 and O_2/N_2 while CO_2/N_2 has a selectivity mostly determined by differences in solubility.

In order to study the effect in diffusivity and solubility selectivities of the different particles used it is better to analyze the corresponding increments of both these selectivities over those for the pure polymeric matrix, which are shown in Table IV. Assuming that, although the absolute errors in these determinations are high, the relative values of the magnitudes between the different membranes should be low, since they have been measured with the same device and under the same measurement conditions. Taking that into account, these values allow stating that:

i. When unmodified γ-alumina particles are added, the diffusivity increases strongly while the changes in solubility are much smaller.

ii. When PVP coated particles are used, the changes are similar to those obtained when the neat γ-alumina particles are used. In this case, diffusivities increase also strongly with a slight increase of solubilities.

iii. Finally in the case of the silanized γ-alumina particles, the changes are much stronger for the solubility that increases for all the gases except methane. On the contrary, diffusivity slightly decreases for all the gases except for methane. This gas shows a relatively strong decrease of both diffusivity and solubility.

The exceptional behaviour of methane can be partly attributed to its size. In effect, it is the biggest molecule among the studied gases as seen in Table III. This could justify the decrease of diffusivity if the free volume of the silane shell consisted in smaller voids than those appearing in the polymeric matrix. The decrease in solubility, in spite of its relatively high critical temperature , could also be explained in terms of a reduction in the size of the voids in such a way that CH_4 could not enter, and thus it is not able to condense in a big proportion of the overall free volume. By the way, this reduction in the size of the voids could also explain the increase in solubility for the other smaller gases because they could enter in the voids easily.

On the other hand, a low chemical compatibility with the silane chains could also explain the decrease of its solubility when silane shells coat the particles. Nevertheless, as shown in Figure 3, the silanized particles, due to the way of their manufacture, have a lower amount of OH groups that those present in both the uncoated and the PVP coated particles. Then, these chains must have more polar character than the silanized ones. Thus, given that methane has the lower polarity among the studied gases, this should in fact lead to an increase in solubility for methane in the mixed matrix containing silanized particles rather than to a decrease as experimentally observed.

4.- Conclusions

The inclusion of nanoparticles of γ-alumina (uncoated, silanized- or PVP-coated) in the *6FDA-6FpDA* polymeric matrix allows an improvement of the permeability versus selectivity trade-off, for all the coatings and pairs of gases used because the resulting mixed-matrix membranes approach the upper bond in the Robeson's plot. Nevertheless, the extension and character of such improvement is different both qualitative and quantitatively for each kind of treatment of the particles and each pair of gases studied.

For all the pairs of gases there are quite similar improvements on gas separation properties but in different directions. In effect increases in permeability are observed when unmodified particles or PVP coated particles are used. While, in the case of mixed matrix membranes incorporating silanized particles, it is the selectivity which increases. Only for the O_2/N_2 pair, the increase in selectivity appearing for the silanized particles is not so effective in advancing towards the Robeson's upper bond when compared with the permeability enhancement registered for the unmodified and PVP coated particles.

It is worth noting that in the case of CO_2/CH_4 the old Robeson's line is crossed because the *6FDA-6FpDA* polymeric matrix gas separation properties were good enough for this pair of gases.

5.- Aknowledgements

Authors are grateful to the support of the Spanish National Plan of RD (projects MAT2005-04976, MAT2008-00619) and to the Junta de Castilla y León (Grupo de Excelencia GR18 and Va088/A08 Project). We are also grateful to the Project I142 Universidad Nacional del Comahue-Argentina and to the Spanish Agency of International Cooperation.

References

1. G.V. Chilingar, J.O. Robertson, S. Kumar, Surface operations in petroleum production, Elsevier, Amsterdam, The Netherlands, 1989

2. J. G. Speight, The chemistry and technology of petroleum, Marcel Dekker, New York, USA, 1999.

3. N.N. Li, A.G.Fane, W.S.W. Ho, T. Matsuura, Advanced Membrane Technology and Applications, Wiley-Interscience, Hoboken, NJ, USA, 2008.

4. S. Van Loo, J. Koppejan, The handbook of biomass combustion and co-firing, Earthscan, London, UK, 2008.

5. P.S. Puri, Gas Separation membranes current status, La Chimica e I´Industria. 78 (1996) 815-821.

6. D.J. Stookey, Gas Separation Membrane Applications, p: 119-150 in “Membrane Technology in the Chemical Industry”, Eds.: S. Pereira-Nunes and K.V. Peinemann, Wiley-VCH, Weinheim, Germany, 2006.

7. J. Marchese, M. Anson, N.A. Ochoa, P. Prádanos, L. Palacio, A. Hernández, Morphology and Structure of ABS Membranes filled with two different Activated Carbons, Chem. Eng. Sci., 61 (2006) 5448-5454.

8. M.L. Cecopieri-Gómez, J. Palacios-Alquisira, J.M. Domínguez, On the limits of gas separation in CO_2/CH_4, N_2/CH_4 and CO_2/N_2 binary mixtures using polyimide membranes, J. Membr. Sci., 293 (2007) 53-65.

9. M. Anson, J. Marchese, E. Garis, N. Ochoa, C. Pagliero, ABS copolymer-activated carbon mixed matrix membranes for CO_2-CH_4 separation, J. Membr. Sci., 243 (2004) 19-28.

10. D.Q. Vu, W. J. Koros, S. J. Miller, Mixed matrix membranes using carbon molecular sieves I. Preparation and experimental results, J. Membr. Sci., 211 (2003) 311-334.

11. D.Q. Vu, W. J. Koros, S.J. Miller, Mixed matrix membranes using carbon molecular sieves II. Modelling permeation behaviour, J. Membr. Sci., 211 (2003) 335-348.

12. C. M. Zimmerman, W. J. Koros, Tailoring mixed matrix composite membranes for gas separations, J. Membr. Sci., 137 (1997) 145-154.

13. S.B. Tartekin-Ersolmaz, C. Atalay-Oral, M. Tather, A. Erdem-Senatalar, B. Schoeman, J. Sterte, Effect of zeolite particle size on the performance of polymer-zeolite mixed matrix membranes, J. Membr. Sci., 175 (2000) 285-288.

14. M.D. Jia, K. V. Peinemann, R. D. Behling, Molecular sieving effect of the zeolite-filled silicone rubber membranes in gas permeation, J. Membr. Sci., 57 (1991) 289-296.

15. T. C. Merkel, Z. He, I. Pinnau, B.D. Freeman, P. Meakin, A.J. Hill, Effect of nanoparticles on gas sorption and transport in poly(1-trimethylsilyl-1-propyne), Macromolecules, 36 (2003) 6844-6855.

16. T. C. Merkel, B. D. Freeman, R. J. Spontak, Z. He, I. Pinnau, P. Meadkin, A. J. Hill, Ultrapermeable, reverse-selective nanocomposite membranes, Science, 296 (2002) 519-520.

17. T.S. Chung, S. S. Chan, R. Wang, Z. Lu, C. He, Characterization of permeability and sorption in Matrimid/C_{60} mixed matrix membranes, J. Membr. Sci., 211 (2003) 91-99.

18. D. Sen, H. Kalıpçılar, L. Yilmaz, Development of polycarbonate based zeolite 4A filled mixed matrix gas separation membranes, J. Membr. Sci. 303 (2007) 194–203

19. S. Matteucci, V. A. Kusuma, S. Swinnea, B. D. Freeman**,** Gas permeability, solubility and diffusivity in 1,2-polybutadiene containing brookite nanoparticles. Polymer 49 (2008) 757-773.

20. Z. He, I. Pinnau, A. Morisato, Nanostructured poly(4-methyl-2-pentyne)/silica hybrid membranes for gas separation, Desalination 146 (2002) 11-15

21. L. Fernández, G. Arranz, L. Palacio, C. Soria, M. Sánchez, G. Pérez, A. E. Lozano, A. Hernández, P. Prádanos, Functionalization of γ-alumina cores by polyvinylpirrolidone: properties of the resulting biocompatible nanoparticles in aqueous suspension, J Nanopart Res, 11 (2009) 341-354.

22. D.W. Van Krevelen, K. te Nijenhuis, Properties of Polymers: Their Correlation with Chemical Structure; Their Numerical Estimation and Prediction from Additive Group Contributions, Elsevier, Amsterdam, The Netherlands, 2009.

23. R. Recio, L. Palacio, P. Prádanos, A.Hernández, A.E. Lozano, A. Marcos, J.G. de la Campa, J. de Abajo, Permeability and selectivity of 6FDA-6FpDA gas membranes prepared from different solvents, Desalination, 200 (2006) 225-226.

24. R. Recio, L. Palacio, P. Prádanos, A.Hernández, A.E. Lozano, A. Marcos, J.G. de la Campa, J. de Abajo, gas separation of 6FDA-6FpDA membranes. Effect of solvent on polymer surfaces and permselectivity, J. Membr. Sci., 293 (2007) 22-28.

25. M. R. Coleman, W. J. Koros, Conditioning of Fluorine-Containing Polyimides. 2. Effect of Conditioning Protocol at 8 % Volume Dilation on Gas-Transport Properties, Macromolecules, 32 (1999) 3106-3113.

26. C. Nagel, K. Günther-Schade, D. Fritsch, T. Strunskus, F. Faupel, Free volume and Transport Properties in Highly Selective Polymer Membranes, Macromolecules, 35 (2002) 2071-2077.

27. K.C. Khulbe, T. Matsuura, G. Lamarche, H.J. Kim, The Morphology Characterisation and Performance of Dense PPO Membranes for Gas Separations, J. Membr. Sci., 135 (1997) 211-223.

28. X. Y. Wang, P.J. in't Veld, Y. Lu, B. D. Freeman, I. C. Sánchez, A molecular Simulation Study of Cavity Size Distribution and Diffusion in *para* and *meta* Isomers, Polymer, 46 (2005) 9155-9161.

29. D.M. Muñoz, J.G. de la Campa, J. de Abajo, A.E. Lozano, Experimental and Theoretical Study of an Improved Activated Polycondensation Method for Aromatic Polyimides, Macromol., 40 (2007) 8225-8232

30. W. Yoshida, R.P. Castro, J.D. Jou, Y. Cohen, Multilayer alkoxysilane silylation of oxide surfaces. Langmuir, 17 (2001) 5882–5888.

31. H.A. Daynes, The process of diffusion through a rubber membrane, Proc. R. Soc. London, 97 (1920) 286-307.

32. D. Paul, A.T. DiBenedetto, Diffusion in amorphous polymers, J. Polym. Sci. C, 10(1) (1965) 17-44.

33. J. Crank, The Mathematics of Diffusion, 2nd Edition,Clarendon Press, Oxford, 1975.

34. R.M. Barrer, G. Skirrow, Transport and equilibrium phenomena in gas-elastomer systems. I. Kinetic phenomena, J. Polym. Sci., 3 (1984) 549-563.

35. W.R. Vieth, Diffusion in and Through Polymers. Principles and Application, Oxford University Press, Hanser, 1991.

36. S.W. Rutherford, D.D. Do, Review of time-lag permeation technique as a method for characterization of porous media and membranes, Adsorption, 3 (1997) 283-312.

37. C. Yeom, B. Kim, and J. Lee. Precise on-line measurements of permeation transients through dense polymeric membranes using a new permeation apparatus. J. Membr. Sci., 161 (1999) 55-66.

38. E. Favre, N. Morliere, and D. Roizard. Experimental evidence and implications of an imperfect upstream pressure step for the time-lag technique. J. Membr. Sci., 207 (2002) 59-72.

39. L. M. Robeson, Correlation of separation factor versus permeability for polymeric membranes, J. Membr. Sci., 62 (1991) 165-185.

40. L.M. Robeson, The upper bound revisited, J. Membr. Sci., 320 (2008) 390–400.

41. S. Matteucci, R. D. Raharjo, V. A. Kusuma, S. Swinnea, B. D. Freeman, Gas Permeability, Solubility, and diffusion Coefficients in 1,2-Polybutadiene Containing Magnesium Oxide, Macromolecules 41 (2008), 2144-2156.

42. S. Matteucci, V. A. Kusuma, D. Sanders, S. Swinnea, B. D. Freeman, Gas transport in TiO_2 nanoparticle-filled poly (1-trimethylsilyl-1-propyne), J. Membr. Sci. 307 (2008) 196–217.

43. T.T. Moore, W.J. Koros, Non-ideal effects in organic–inorganic materials for gas separation membranes, J. Molecular Structure, 739 (2005) 87–98.

44. T. S. Chung, L. Y. Jiang, Y. Li, S. Kulprathipanja, Mixed matrix membranes (MMMs) comprising organic polymers with dispersed inorganic fillers for gas separation, Progress Polym. Sci., 32, 483-507 (2007).

45. Y. Li, T.S. Chung, C. Cao, S. Kulprathipanja, The effects of polymer chain rigidification, Zeolite pore size and pore blockage on polyethersulfone (PES)-zeolite A mixed matrix membranes, J. Membr. Sci., 260 (2005) 45

46. N. Widjojo, T. S. Chung, S. Kulprathipanja, The fabrication of hollow fiber membranes with double-layer mixed-matrix materials for gas separation, J. Membr., Sci. 325, 326-335 (2008).

47. R. Recio, A. E. Lozano, P. Pradanos, A. Marcos,.F. Tejerina, A. Hernandez, Effect of Fractional Free Volume and Tg on Gas Separation Through Membranes Made with Different Glassy Polymers, J. Applied Polymer Science, 107 (2008) 1039–1046.

48. M. Sadeghi, M.A. Semsarzadeh, H. Moadel, Enhancement of the gas separation properties of polybenzimidazole (PBI) membrane by incorporation of silica nano particles, J. Membr. Sci., 331 (2009) 21-30.

49. J. Marchese, E. Garis, M. Anson, N. A. Ochoa, C. Pagliero, Gas sorption, permeation and separation of ABS copolymer membrane, J. Membr. Sci., 221, (2003) 185-197.

50. D. W. Breck, Zeolite molecular sieves: structure, chemistry and use, Wiley, New York, NY, 1974.

FIGURE CAPTION

Fig. 1.- Chemical structure of the 6FDA-6FpDA

Fig. 2.- Silylation reaction (A), hydrolysis of metoxy groups (B) and polymerization reaction (C).

Fig. 3.- Sketch of the particles used and their coating layer showing the chemical structure on their surfaces.

Fig. 4.- SEM images of cross sections of the membranes studied.

Fig. 5.- Diagram of the permeation device: 1. Gas supply, 2. Pressure regulator, 3. Quick connection, 4. Gas reservoir, 5. Relief valve, 6. High pressure transducer, 7. Permeation cell, 8. Expansion cylinder, 9. Relief valve, 10. Low pressure transducer, 11. Turbo-molecular pump, 12. Rotary pump, 13. Power source, 14. Data acquisition.

Fig. 6.- An example of the time lag plots obtained.

Fig.7.- Robeson's plots for the gas pairs: CO_2/CH_4 (A) O_2/N_2 (B) N_2/CH_4 (C) and CO_2/N_2 (D). The 1991 (when existing) and 2008 Robeson's bonds are shown. The big crossed circle corresponds to the polymeric matrix alone. Also a dashed line is drawn in parallel to these bond lines but passing close to the experimental points to help judging how the use of each particle improves the membrane results.

Fig. 8.- Diffusivity versus the kinetic diameter for the gases and membranes used (A) and Solubility versus the critical temperature for the gases and membranes used (B).

Fig. 9.- *S*olubility selectivity versus the diffusivity selectivity for all the membranes and gas pairs studied. Note that over the diagonal the membrane selectivity is more determined by solubility than by diffusivity and the other way round below the diagonal.

TABLES

Table I: Specific surface areas and particle diameters

Treatment	**S_S (m^2/g)**	**d_p (nm)**
Unmodified particles of alumina	37.75	39.72
Silanized alumina	29.29	51.20
PVP coated particles	25.70	177.4

Table II: Manufactured membranes with similar w/w percentages of differently treated particles.

Membrane	**6F6FpDA weight (g)**	**Weight of particles (g)**	**% w/w**
Unmodified particles of alumina	0.5998	0.0805	11.83
Silanized alumina	0.6022	0.0800	11.72
PVP coated particles	0.6090	0.0795	11.54

Table III: Kinetic diameters and critical temperature of the used gases.

Gas	**CO_2**	**O_2**	**N_2**	**CH_4**
Kinetic diameter, d_c (Å)	3.30	3.46	3.64	3.80
Critical temperature, T_c (K)	304.4	154.790	126.2	190.6

Table IV: Change in diffusivity and selectivity of all the gases studied referred to that of the 6FDA-6FPDA when the different γ-alumina particles are included in the polymeric matrix.

Changes in Diffusivity referred to that of the polymeric matrix (%)				
γ-alumina particles	CO_2	O_2	N_2	CH_4
Unmodified	48.7	61.3	31.9	29.3
Silanized	-2.8	-0.8	-3.4	-7.0
PVP coated	55.9	30.7	35.2	36.6
Changes in Solubility referred to that of the polymeric matrix (%)				
γ-alumina particles	CO_2	O_2	N_2	CH_4
Unmodified	2.7	-7.9	13.4	0.8
Silanized	16.9	12.8	14.9	-8.0
PVP coated	-2.2	15.7	10.2	-3.2

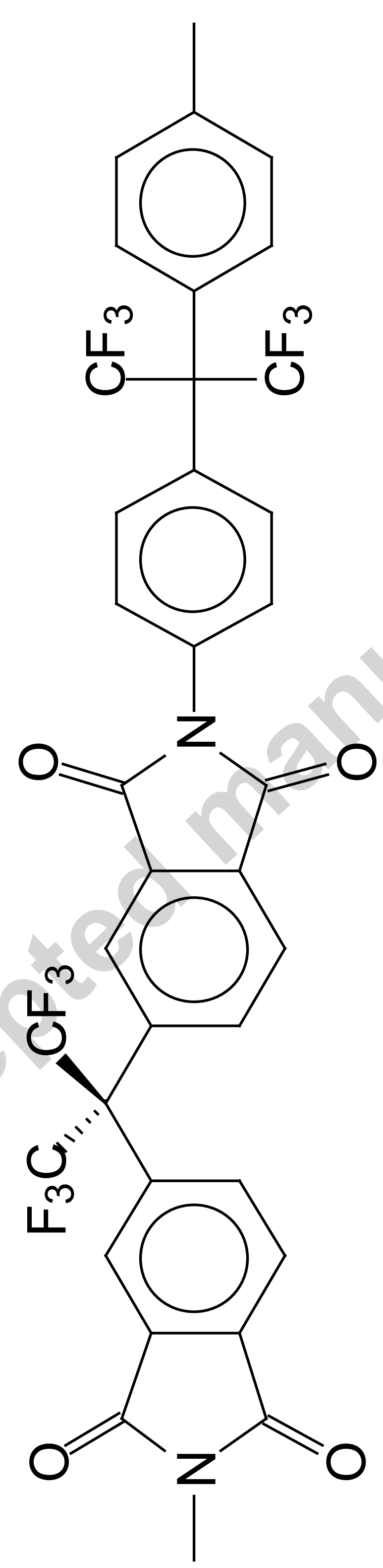

Fig. 1

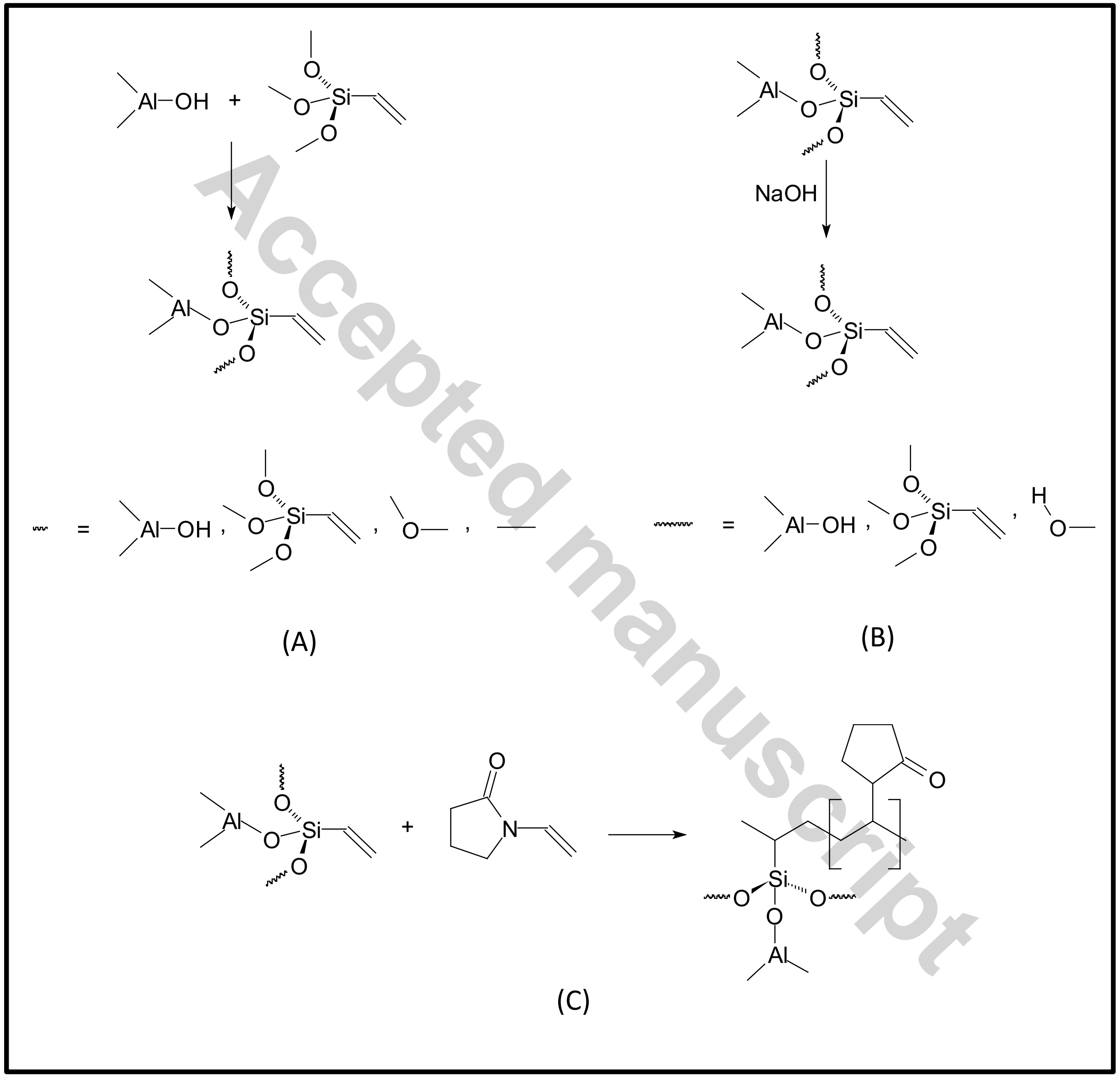

Fig. 2

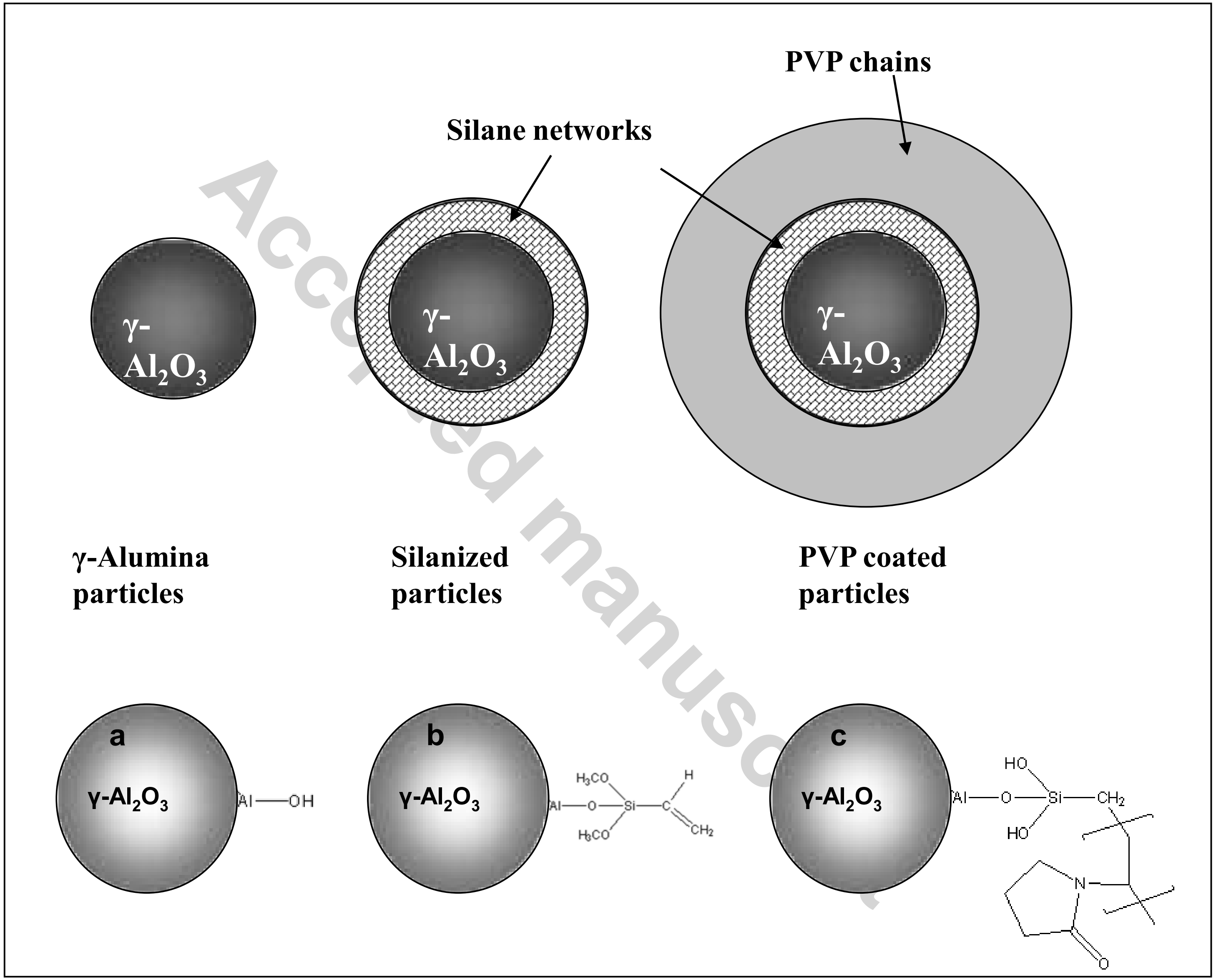
PVP chains
Silane networks
γ-Al2O3
γ-Al2O3
γ-Al2O3
γ-Alumina particles
Silanized particles
PVP coated particles
a
b
c
γ-Al2O3
γ-Al2O3
γ-Al2O3
Al—OH
H3CO
H
Al—O—Si—C
H3CO
CH2
HO
Al—O—Si—CH2
HO
N
O

Fig. 3

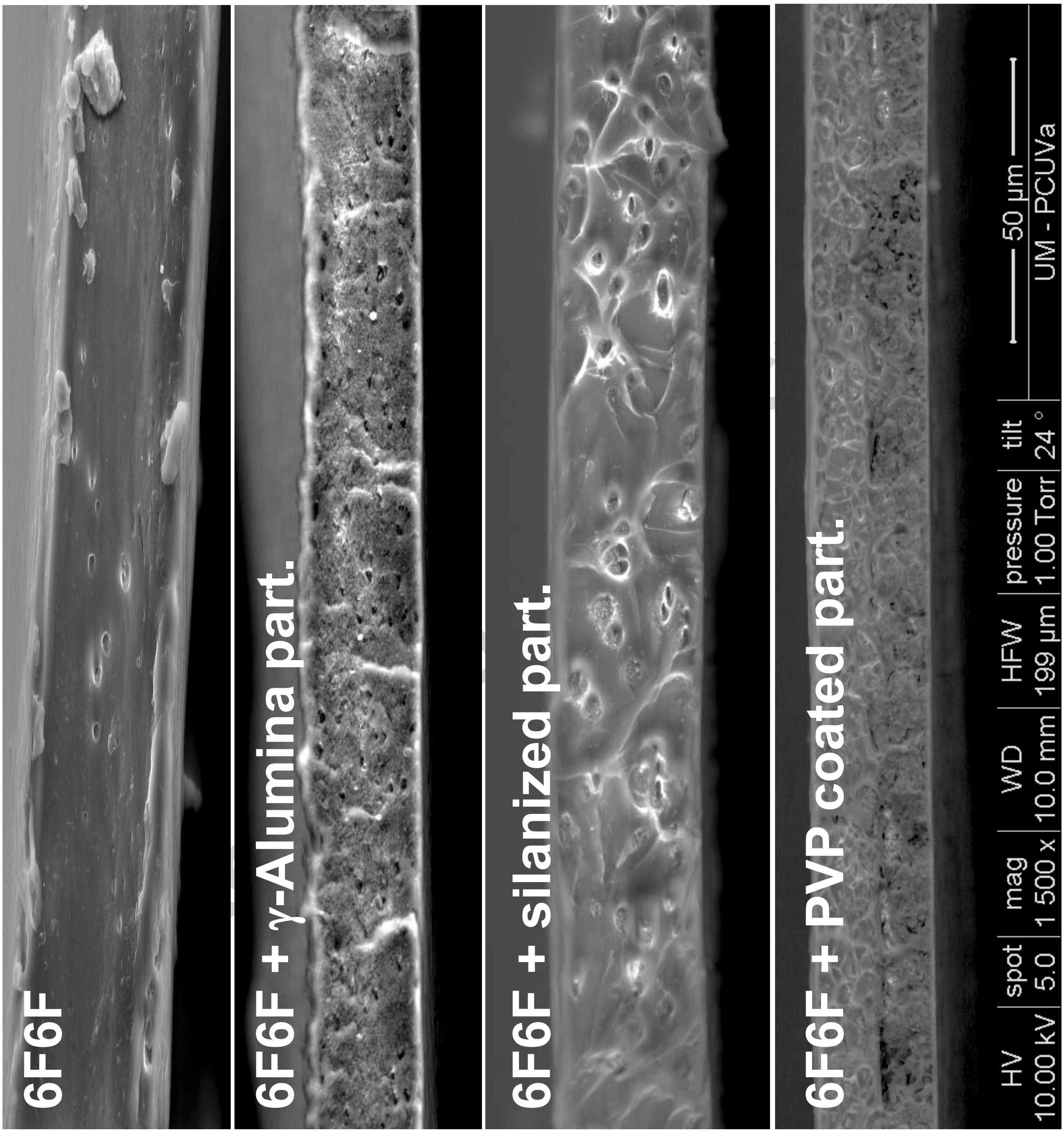
6F6F
6F6F + γ-Alumina part.
6F6F + silanized part.
6F6F + PVP coated part.
HV 10.00 kV
spot 5.0
mag 1 500 x
WD 10.0 mm
HFW 199 μm
pressure 1.00 Torr
tilt 24 °
50 μm
UM - PCUVa

Fig. 4

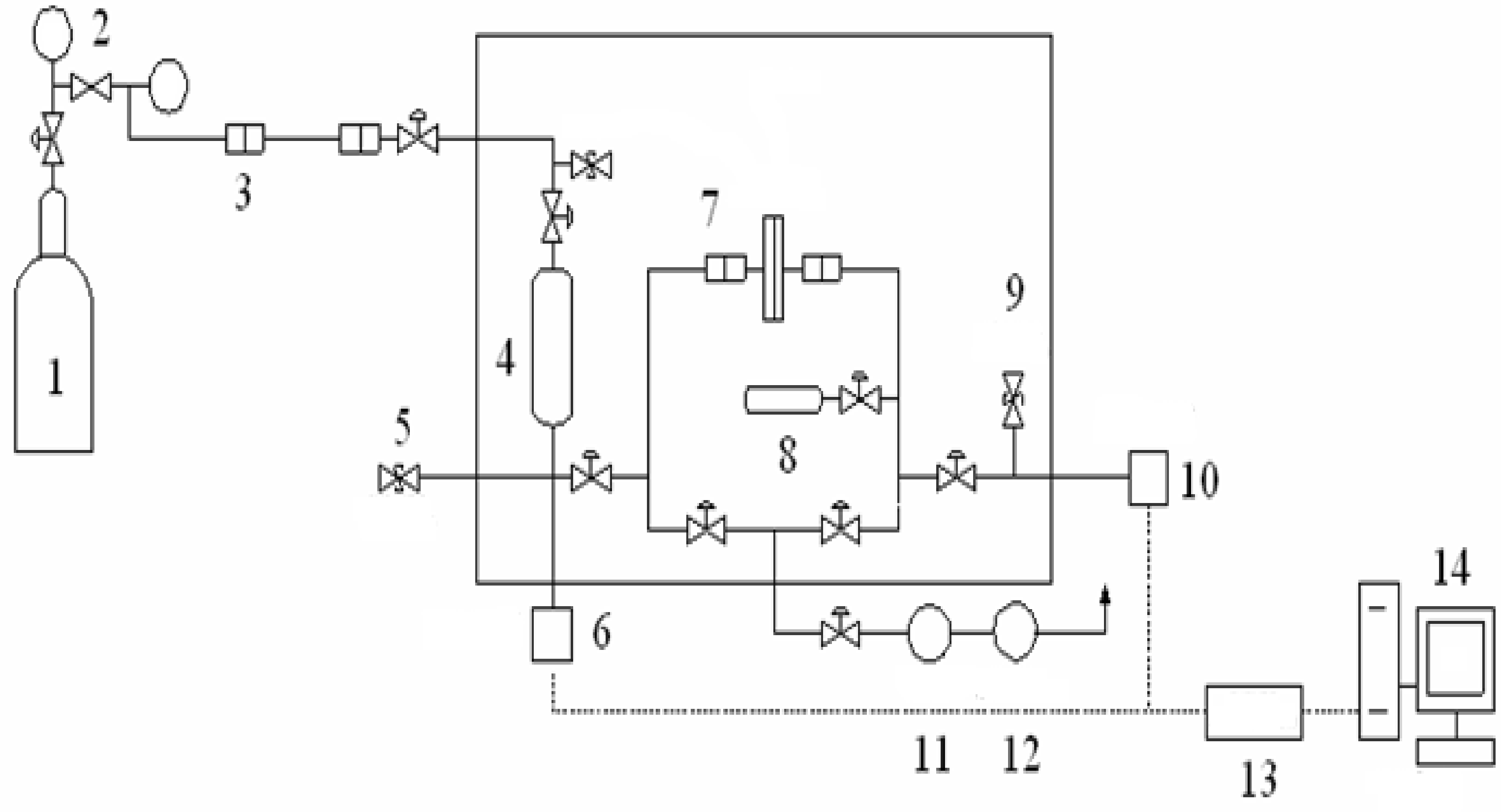

Fig. 5

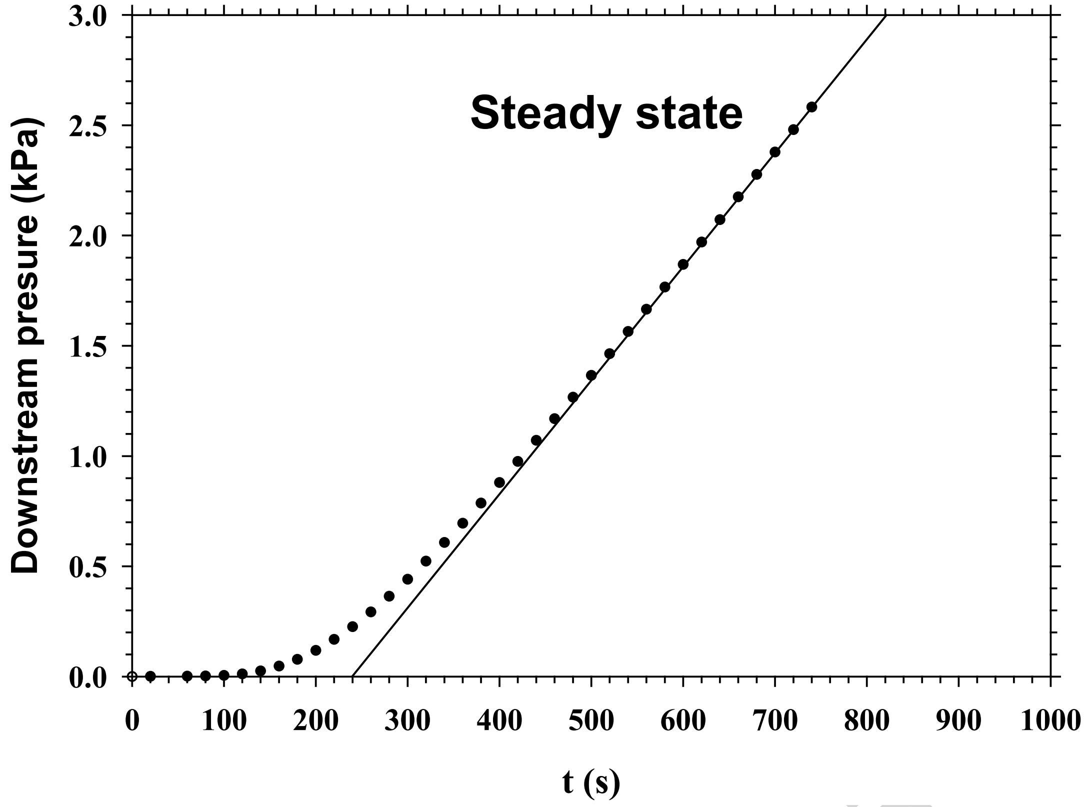
Steady state
Downstream presure (kPa)
0.0
0.5
1.0
1.5
2.0
2.5
3.0
0
100
200
300
400
500
600
700
800
900
1000
t (s)

Fig. 6

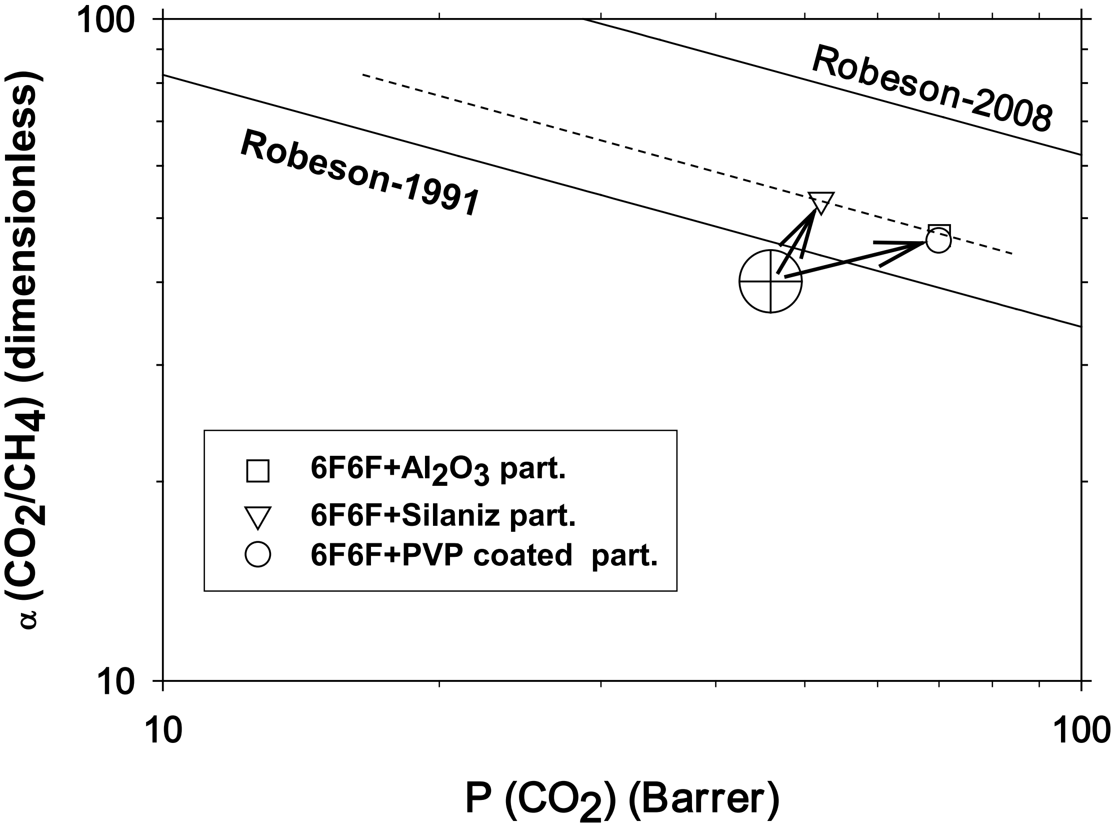
100
10
10
100
Robeson-2008
Robeson-1991
□ 6F6F+Al_2O_3 part.
▽ 6F6F+Silaniz part.
○ 6F6F+PVP coated part.
α (CO_2/CH_4) (dimensionless)
P (CO_2) (Barrer)

Fig. 7-A

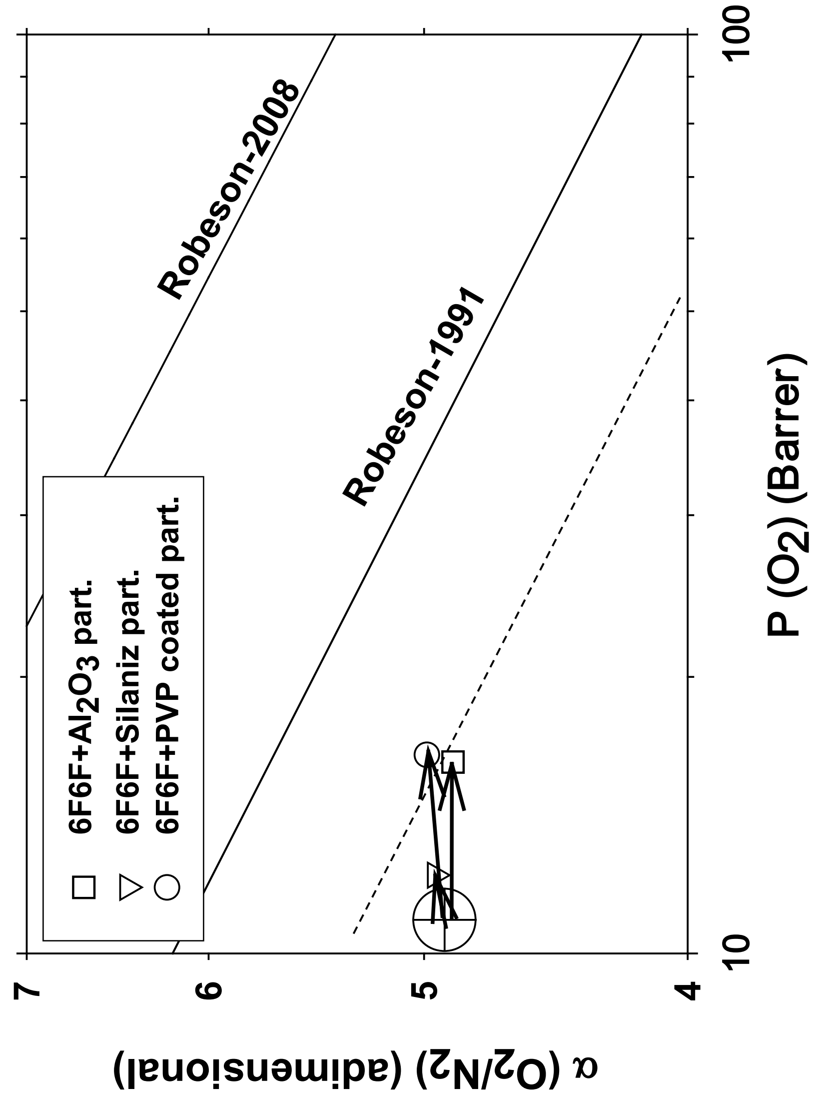
α (O$_2$/N$_2$) (adimensional)
P (O$_2$) (Barrer)
7
6
5
4
10
100
Robeson-2008
Robeson-1991
□ 6F6F+Al$_2$O$_3$ part.
▷ 6F6F+Silaniz part.
○ 6F6F+PVP coated part.

Fig. 7-B

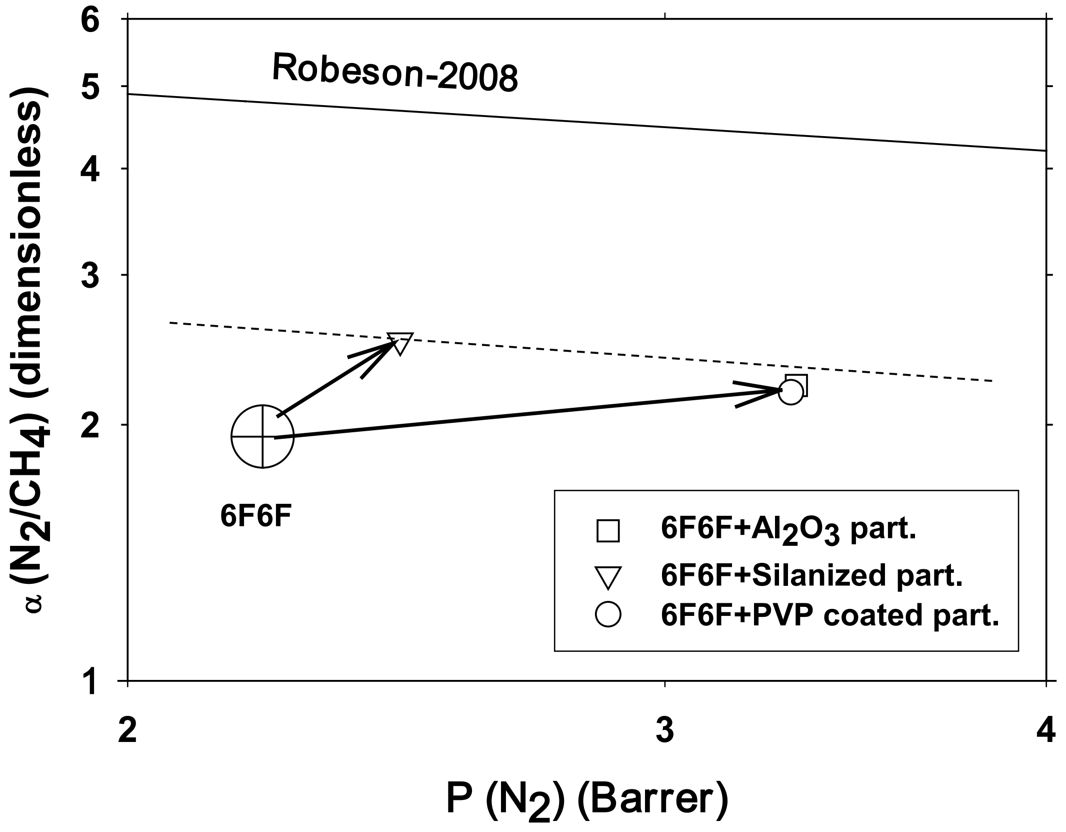
6
5
4
3
2
1
2
3
4
α (N2/CH4) (dimensionless)
P (N2) (Barrer)
Robeson-2008
6F6F
6F6F+Al2O3 part.
6F6F+Silanized part.
6F6F+PVP coated part.

Fig. 7-C

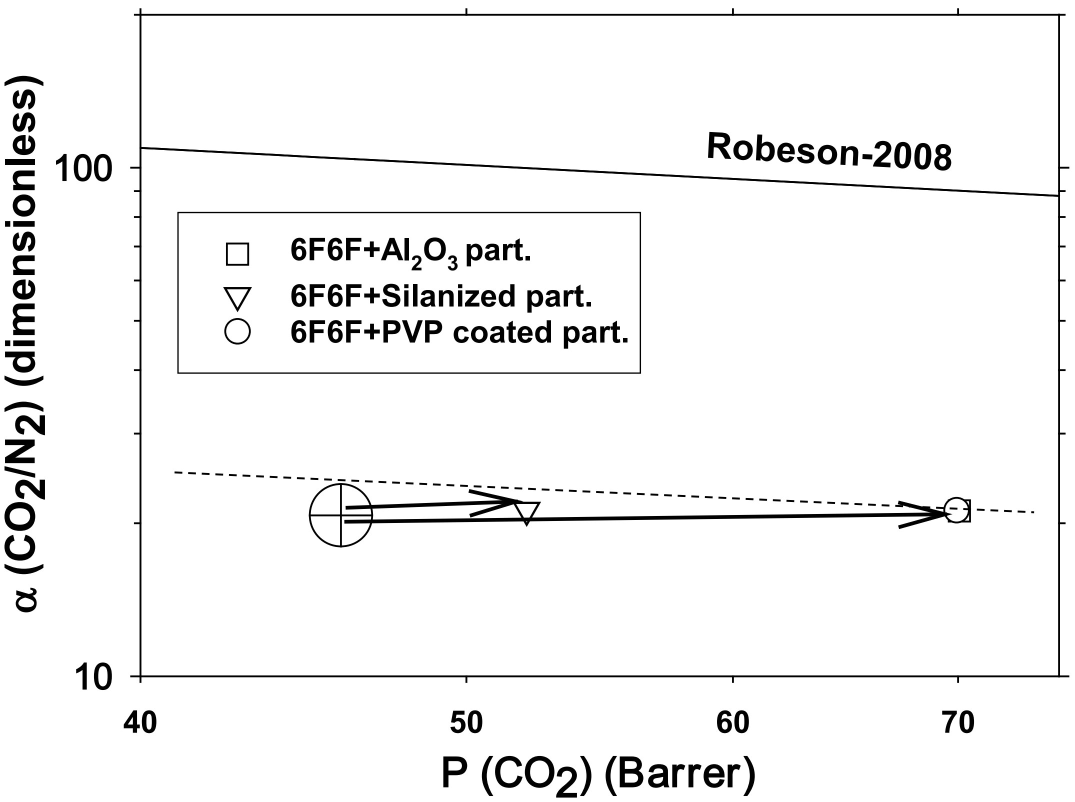
Robeson-2008
6F6F+Al_2O_3 part.
6F6F+Silanized part.
6F6F+PVP coated part.
α (CO_2/N_2) (dimensionless)
100
10
40
50
60
70
P (CO_2) (Barrer)

Fig. 7-D

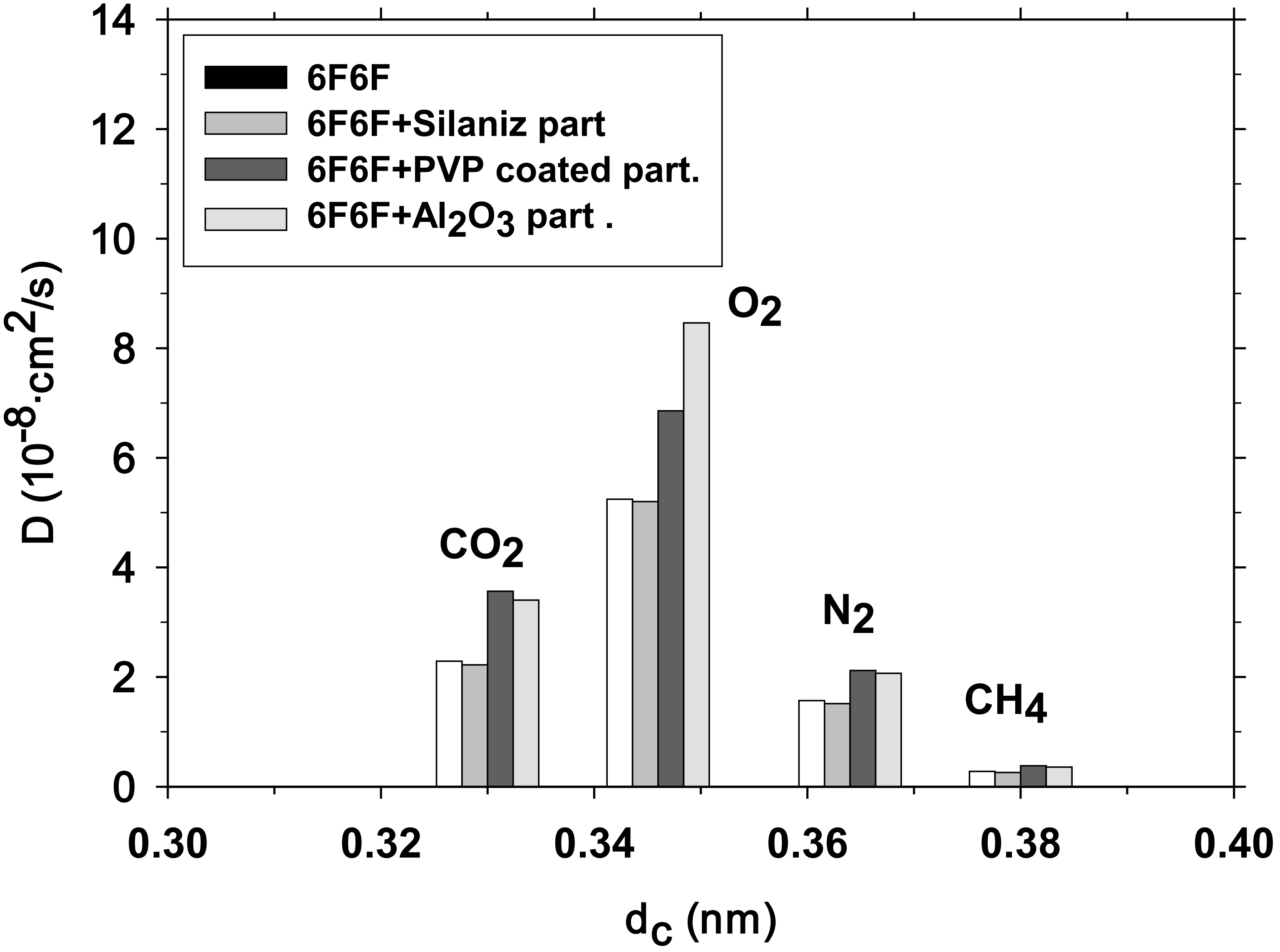
6F6F
6F6F+Silaniz part
6F6F+PVP coated part.
6F6F+Al_2O_3 part .
O_2
CO_2
N_2
CH_4
D (10^{-8}.cm^2/s)
0
2
4
6
8
10
12
14
0.30
0.32
0.34
0.36
0.38
0.40
d_C (nm)

Fig. 8-A

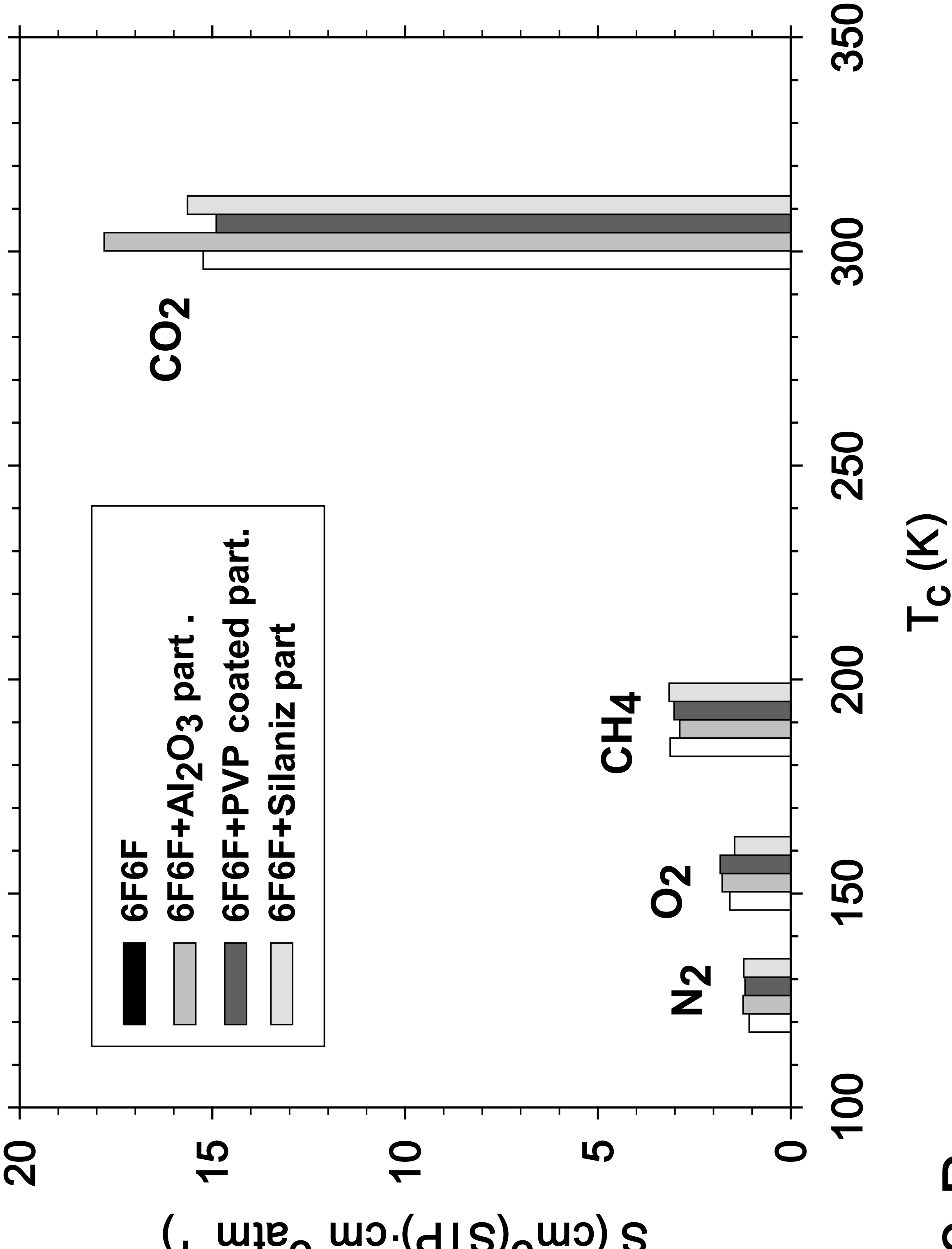
S (cm^3(STP)·cm^{-3}atm^{-1})
0
5
10
15
20
T$_C$ (K)
100
150
200
250
300
350
N$_2$
O$_2$
CH$_4$
CO$_2$
6F6F
6F6F+Al$_2$O$_3$ part .
6F6F+PVP coated part.
6F6F+Silaniz part

Fig. 8-B

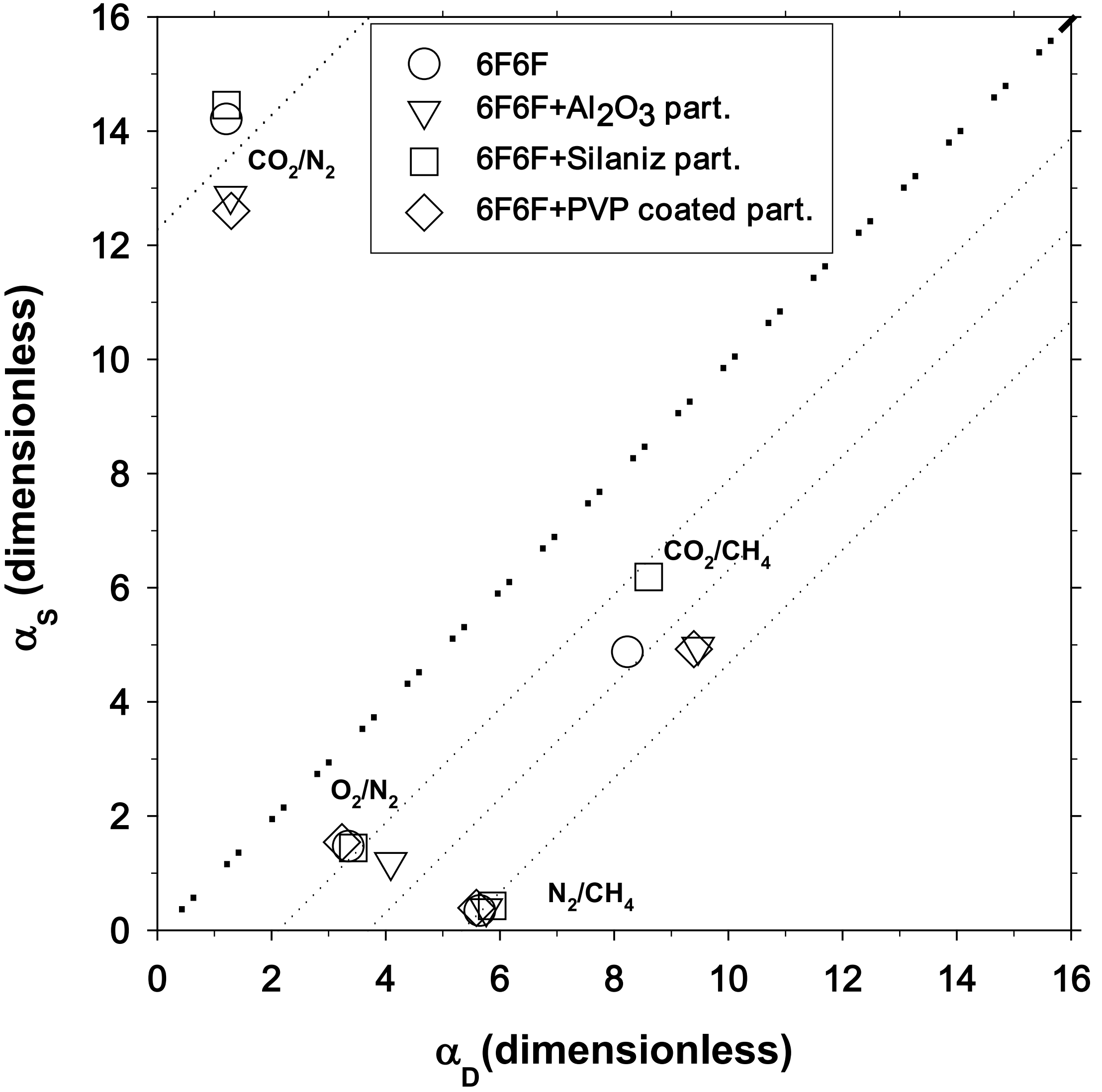
6F6F
6F6F+Al2O3 part.
6F6F+Silaniz part.
6F6F+PVP coated part.
CO2/N2
O2/N2
CO2/CH4
N2/CH4
αS (dimensionless)
αD(dimensionless)
0
2
4
6
8
10
12
14
16

Fig. 9